Nuclear Engineering and Technology 48 (2016) 33–42

Available online at ScienceDirect

Nuclear Engineering and Technology

journal homepage: www.elsevier.com/locate/net

Original Article

A Study of Neutronics Effects of the Spacer Grids in a Typical PWR via Monte Carlo Calculation

Xuan Bach Tran [1] *and Nam Zin Cho* [*]

Korea Advanced Institute of Science and Technology, 291 Daehak-ro, Yuseong-gu, Daejeon 34141, South Korea

ARTICLE INFO

Article history:
Received 11 February 2015
Received in revised form
9 September 2015
Accepted 10 September 2015
Available online 19 October 2015

Keywords:
Banded Dissolution Spacer Grids Modeling
Volume-preserving Streamlined Heterogeneous Spacer Grids

ABSTRACT

Spacer grids play an important role in maintaining the proper form of the fuel assembly structure and ensuring the safety of reactor core design. This study applies the Monte Carlo method to the analysis of the neutronics effects of spacer grids in a typical pressurized water reactor (PWR). The core problem used to analyze the neutronics effects of spacer grids is a modified version of Korea Advanced Institute of Science and Technology benchmark problem 1B, based on an Advanced Power Reactor 1400 (APR1400) core model. The spacer grids are modeled and added to this test problem in various ways. Then, by running MCNP5 for all cases of spacer grid modeling, some important numerical results, such as the effective multiplication factor, the spatial distributions of neutron flux, and its energy spectrum are obtained. The numerical results of each case of spacer grid modeling are analyzed and compared to assess which type has more advantages in accuracy of numerical results and effectiveness in terms of geometry building. The conclusion is that the most realistic modeling for Monte Carlo calculation is the "volume-preserving" streamlined heterogeneous spacer grids, but the "banded" dissolution spacer grids modeling is a more practical yet accurate model for routine (deterministic) analysis.

1. Introduction

The reactor design process is significantly affected by the design and distribution of fuel assemblies inside the core. Therefore, safety in the design of a reactor greatly depends on the accuracy of neutronics calculations in fuel assembly design. Among the most important structural components in a fuel assembly, the spacer grid plays a major role in supporting the fuel rods laterally and vertically.

This research focuses on applying the Monte Carlo method to the analysis of the effects of spacer grids, and on producing numerical results of neutronics calculations in a typical PWR. The spacer grids are added to assemblies of the test problem according to three ways of modeling: "volume-preserving"

* *Corresponding author.*
E-mail address: nzcho@kaist.ac.kr (N.Z. Cho).

[1] Current address: Ministry of Science and Technology, 113 Tran Duy Hung Street, Hanoi, Vietnam.

http://dx.doi.org/10.1016/j.net.2015.10.001
1738-5733/

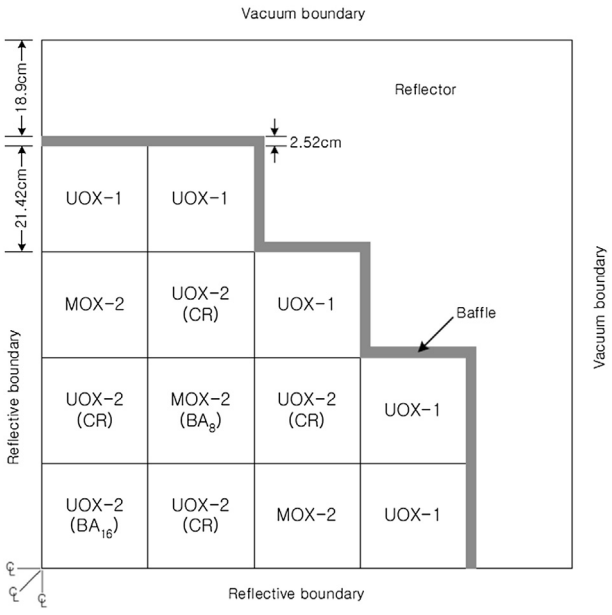

Fig. 1 – Horizontal cut of KAIST benchmark problem 1B. KAIST, Korea Advanced Institute of Science and Technology.

streamlined heterogeneous, bulk dissolution, and banded dissolution modeling. Then, the effective multiplication factor, spatial distributions of neutron flux, and its energy spectrum are compared. Numerical results show that the effects of spacer grids are not negligible. In addition, some comparisons are provided between a case which does not include the spacer grids and cases which do include the spacer grids. From these comparison results, it is possible to assess how spacer grids affect neutronics calculations in the reactor, and which spacer grid modeling method should be used with acceptable accuracy and simplicity to describe the real geometry.

The MCNP5 [1] is applied as a tool for building the geometry of a test problem as well as the spacer grids and for obtaining numerical results. The data for the spacer grid used in this research is taken from some basic data from the spacer grid model of the PLUS7 fuel [2], developed by Korea Electric Power Corporation (KEPCO; Naju, Korea) and Westinghouse (Pittsburgh, PA, USA). A similar study on the effects of various spacer grid models was performed based on the VVER-1000 reactor [3].

This article is arranged into three main parts. Section 2 shows how the spacer grids are modeled and added to the test problem. In Section 3, the main numerical results obtained from the output of MCNP5 are displayed and analyzed. Finally, a summary and the conclusions of the study are presented in Section 4.

2. Test problem and spacer grid modeling description

In this section, the geometry of the test problem and the spacer grids modeling methods are described.

2.1. *Test problem (without spacer grids)*

The test problem used for the analysis in this study is a modified version of the Korea Advanced Institute of Science and Technology (KAIST) benchmark problem 1B [4] based on the Advanced Power Reactor 1400 (APR1400) core model in which MOX fuel is loaded into a small PWR core as shown in Fig. 1.

This benchmark problem is modified by adding upper and lower structure materials to the active core region. These upper and lower structures are built by mixing SS-304 and light water (H_2O) in certain proportions [5]. In addition, the model of the downcomer and reactor vessel, which are applied in the APR1400 core model, are also added to the

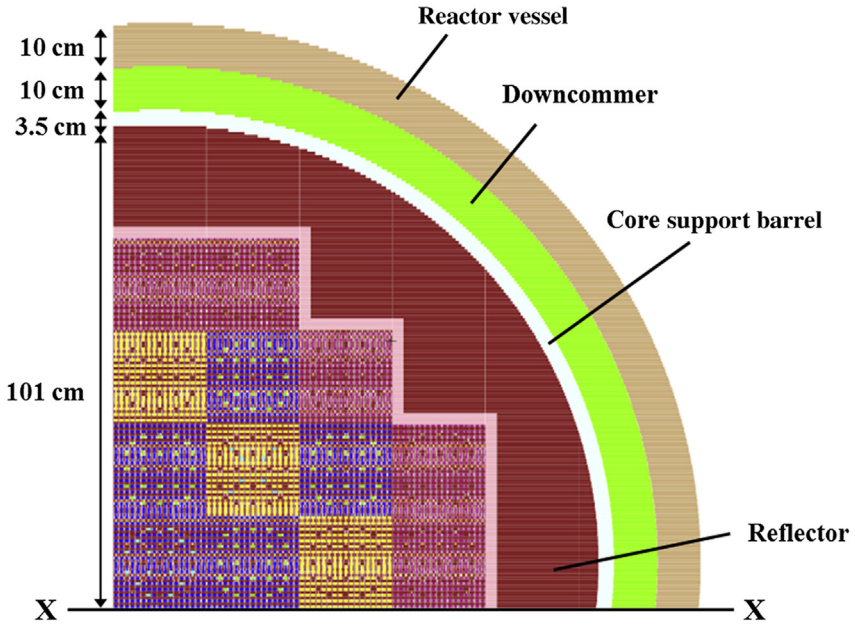

Fig. 2 – Horizontal cut of the test problem colored by material.

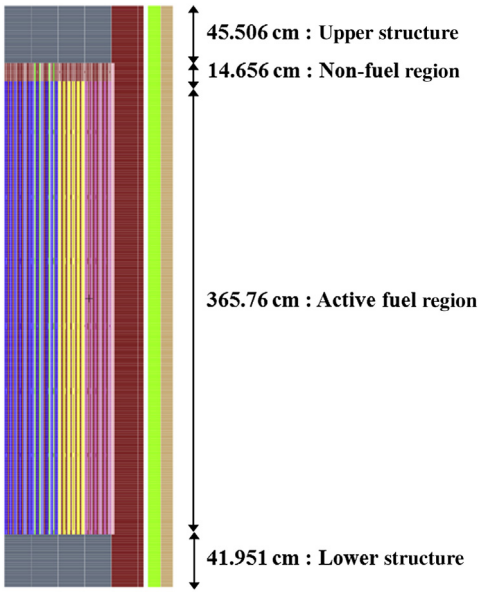

Fig. 3 – Vertical cut of the test problem (X-X cross section) colored by material.

problem geometry. Depending on the appropriate proportion of the core size, the radius of the downcomer and reactor vessel were set as 1/2 the real radius of those in the APR1400 core. The downcomer is filled with cold H_2O, the core support barrel and the vessel materials are SA-182 and SA-508, respectively. Using MCNP5, the geometry of the test problem without spacer grids is built as in Figs. 2 and 3.

2.2. *Modeling of spacer grids*

Spacer grids are added to the aforementioned geometry using three types of modeling: a "volume-preserving" streamlined heterogeneous model, a bulk dissolution model, and a banded dissolution model. The detailed processes of these types of modeling will be explained in this section.

All specifications of the spacer grid in this study are taken from the basic technical parameters of the advanced spacer grid design of the PLUS7 fuel. Each assembly contains eight spacer grids (2 end grids and 6 intermediate grids) along the assembly length. The axial locations of these spacer grids are shown in Table 1 [6].

The material composition of the spacer grids is presented in Table 2 below.

Table 1 – Geometrical specifications of spacer grids.

	End grids	Intermediate grids
Number	2	6
Height (cm)	3.723	4.1148
Axial locations (cm) (center of spacer grids to top of lower structure)	13.884 388.2	75.2 127.4 179.6 231.8 284.0 336.2

Table 2 – Material composition of spacer grids (Zircaloy–4).

Isotope	Atom density (10E+24 cm^{-3})	Isotope	Atom density (10E+24 cm^{-3})
Zr-90	2.18865E-02	Fe-54	8.68307E-06
Zr-91	4.77292E-03	Fe-56	1.36306E-04
Zr-92	7.29551E-03	Fe-57	3.14789E-06
Zr-94	7.39335E-03	Fe-58	4.18926E-07
Zr-96	1.19110E-03	Cr-50	3.30121E-06
Sn-112	4.68066E-06	Cr-52	6.36606E-05
Sn-114	3.18478E-06	Cr-53	7.21860E-06
Sn-115	1.64064E-06	Cr-54	1.79686E-06
Sn-116	7.01616E-05	Hf-174	3.54138E-09
Sn-117	3.70592E-05	Hf-176	1.16423E-07
Sn-118	1.16872E-04	Hf-177	4.11686E-07
Sn-119	4.14504E-05	Hf-178	6.03806E-07
Sn-120	1.57212E-04	Hf-179	3.01460E-07
Sn-122	2.23417E-05	Hf-180	7.76449E-07
Sn-124	2.79392E-05		

2.2.1. *Volume-preserving streamlined heterogeneous model*

In this type of modeling, the spacer grids are built with a geometry similar to reality. Fig. 4 [7] shows the typical geometry of a spacer grid in a PWR. To avoid the nonstandard curved geometry of the spacer grids while maintaining their heterogeneity so they can be easily handled by MCNP5, the shape of the spacer grid is simplified with a preserving mass, where its configuration around a single fuel rod is shown in Fig. 5.

2.2.2. *Bulk dissolution model*

In this modeling process, the spacer grids are "dissolved" with the moderator in *the whole core* (from the bottom part to the upper part). The dissolved material is then a mixture of spacer grid materials and the moderator (which contains boron and light H_2O). The volume, mass, and density of the *new materials mixture* are obtained by these formulas:

$$V_{new} = V_{grid} + V_{mod}, \quad (1)$$

$$m_{new} = m_{grid} + m_{mod}, \quad (2)$$

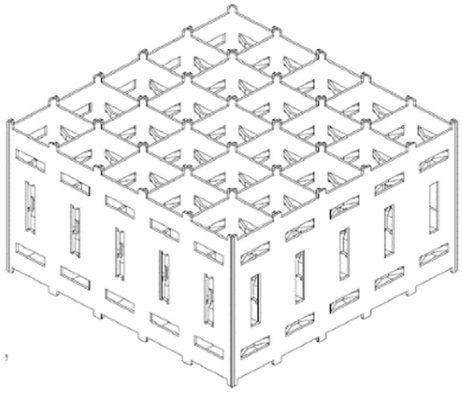

Fig. 4 – Real geometry of a spacer grid.

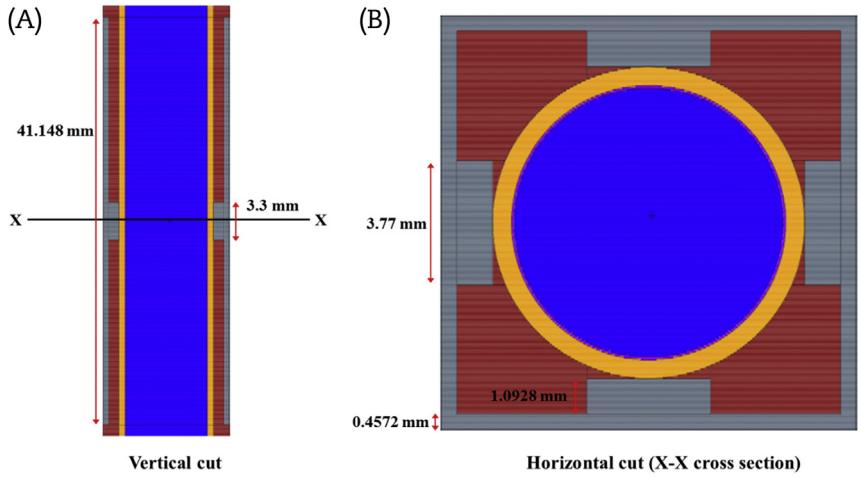

Fig. 5 – Vertical cut (left) and horizontal cut (right) of the "volume-preserving" streamlined heterogeneous spacer grid.

$$\rho_{new} = m_{new}/V_{new}, \quad (3)$$

where V_{new}, V_{grid}, V_{mod}, m_{new}, m_{grid}, m_{mod}, and ρ_{new} are total volume, mass, and density of new material mixture, spacer grids, and moderator, respectively. These equations are used to derive the summary data shown in Table 3.

2.2.3. *Banded dissolution model*

Implementing the same process as in the bulk dissolution modeling, the spacer grid materials are "dissolved" into the moderator but only around eight specific locations of spacer grids (not the moderator of the whole core) are introduced in Table 1. The limitation of the axial length of these eight regions is the axial length of each spacer grid (4.1148 cm).

The total mass and volume of the spacer grids are kept the same as in the "volume-preserving" streamlined heterogeneous model and bulk dissolution model. The total mass and volume of the moderator used to mix with the spacer grids are calculated again with the new axial length of 4.1148 cm. Applying the same process as in the bulk dissolution model, the mass, volume, and density of the new material mixture are obtained, as shown in Table 4. Note that the dissolution models (bulk and banded) could be analyzed by deterministic methods.

3. Numerical results and analysis

Using MCNP5, the multiplication factor, axial, and radial flux distributions are obtained for the following four cases: Case 1, test problem without any spacer grids; Case 2, test problem with est problem withhou streamlined heterogeneous spacer grids; Case 3, test problem with bulk dissolution spacer grids; and Case 4, test problem with banded dissolution spacer grids.

For all cases, 300,000 histories/cycle, 300 inactive cycles, and 300 active cycles are used.

In all analyses of this study, the results from Case 2 are used as a reference to make comparisons with the results from the other remaining cases, because in Case 2 the geometry of the spacer grids model is the closest to reality. Therefore, the results of Case 2 could be considered to have the highest accuracy in terms of reflecting the effects of spacer grids, compared with the results of the other two "spacer grid" cases (Case 3 and Case 4).

3.1. *Effective multiplication factor*

As shown in Table 5, Case 1 which does not include spacer grids, shows the highest multiplication factor ($k_{eff} = 0.977610$) compared to the remaining cases. This is because the volume of the spacer grids (Zircaloy-4) are replaced with H_2O in Case 1, where H_2O moderates neutrons more effectively than spacer grids. Case 3, which contains bulk dissolution spacer grids, has the next highest multiplication factor, followed by Case 4, which includes banded dissolution spacer grids. Case 2, in which spacer grids are described with the most detailed geometry, provides the lowest multiplication factor. The difference in the multiplication factors between Case 4 and Case 2 is 117 pcm, whereas the difference between Case 3 and Case 2 is

Table 3 – Mass, volume, and density of bulk dissolution material.

	Total mass (g)	Total volume (cm^3)	Density (g/cm^3)
Spacer grids	227,150.7286	34,626.63546	6.56
Moderator	940,151.2793	1,288,761.178	0.7295
New mixing material	1,323,387.813	1,167,302.008	0.882

Table 4 – Mass, volume, and density of banded dissolution model.

	Total mass (g)	Total volume (cm^3)	Density (g/cm^3)
Spacer grids	227,150.7286	34,626.63546	6.56
Moderator	101,426.1	139,035.0476	0.7295
New mixing material	328,576.8	173,661.683	1.8920512

Table 5 – Comparison of multiplication factors.

	k_{eff} (Standard deviation)	Difference from Case 2[b]
Case 1[a]	0.97761 (0.00008)	0.00399
Case 2[b]	0.97362 (0.00008)	–
Case 3[c]	0.97706 (0.00008)	0.00344
Case 4[d]	0.97479 (0.00008)	0.00117

[a] Test problem without any spacer grids.
[b] Test problem with "volume-preserving" streamlined heterogeneous spacer grids.
[c] Test problem with bulk dissolution spacer grids.
[d] Test problem with banded dissolution spacer grids.

344 pcm. Thus, the multiplication factor increases, as the spacer grids are dissolved in the moderator more uniformly.

3.2. *Horizontal neutron flux distribution*

Fig. 6A and 6B provide, for Case 4, the pinwise radial neutron flux distributions at the grid plate (from z = 178.0542 to z = 182.169) and nongrid plate (from z = 173.9394 to z = 178.0542), respectively, whereas Fig. 6C shows the ratio of pinwise flux distributions at the nongrid plate to those at the grid plate. Note that z = 0 at the top of the lower structure. Although the grid plate is closer to the center of the active fuel region, pinwise flux distributions at the grid plate are lower than those at the nongrid plate in "fuel assembly regions". In the reflector regions, however, this tendency is not clearly seen due to the stochastic errors in flux tallies.

3.3. *Axial power distribution of center assembly*

Fig. 7 shows the axial power distributions in the center assembly for four cases. The linear power density in the four cases is normalized by the total power of the core (900 MWth). The axial power shape of Case 2 is not as smooth as that of Case 1. This is caused by the appearance of spacer grids along the length of the assembly. At each point where the moderator is replaced by a spacer grid, the linear power density decreases because, as mentioned previously, the replacement of the moderator by spacer grid materials decreases the number of

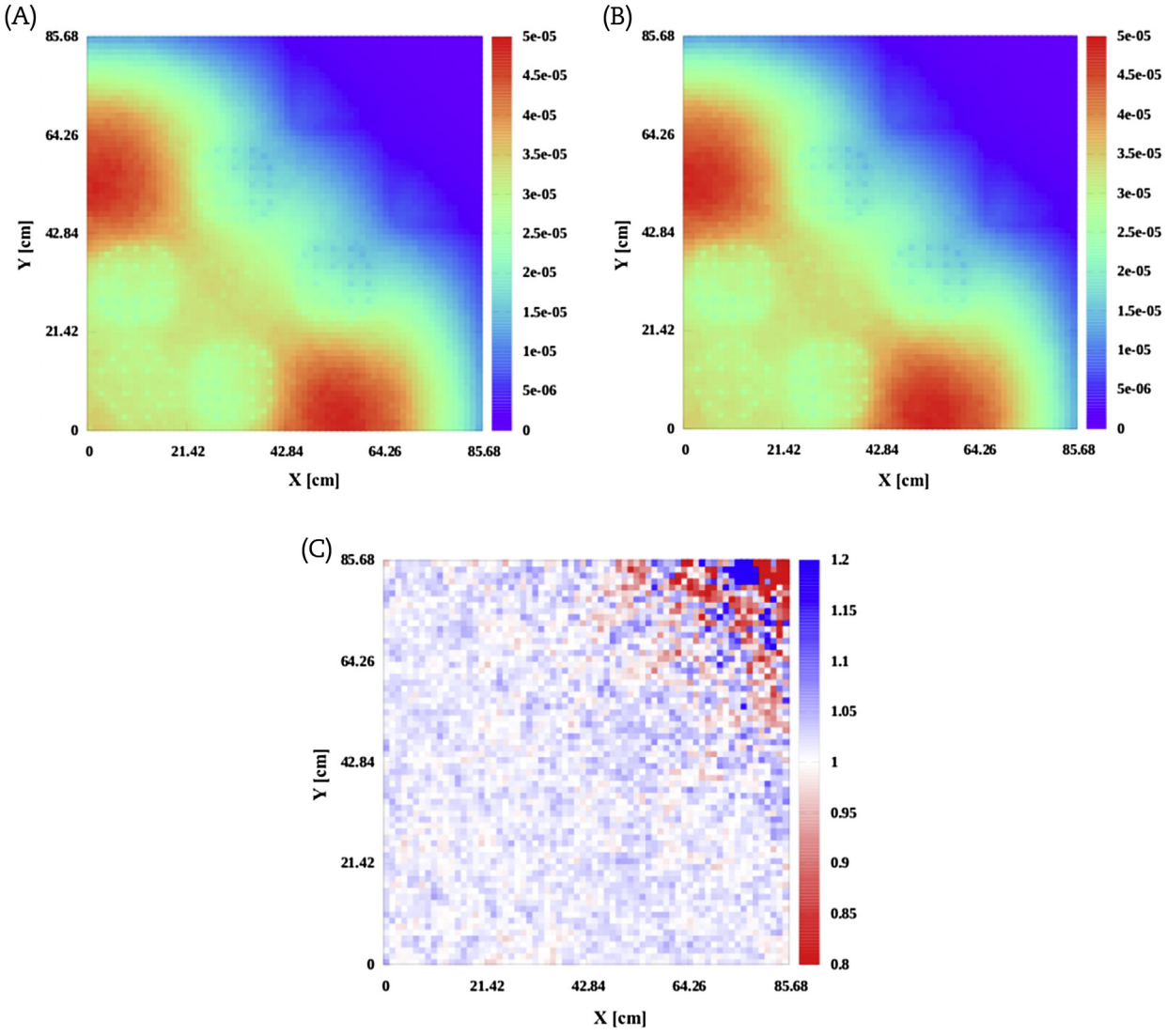

Fig. 6 – Pinwise neutron flux distributions for Case 4 (z = 0 at the top of lower structure).

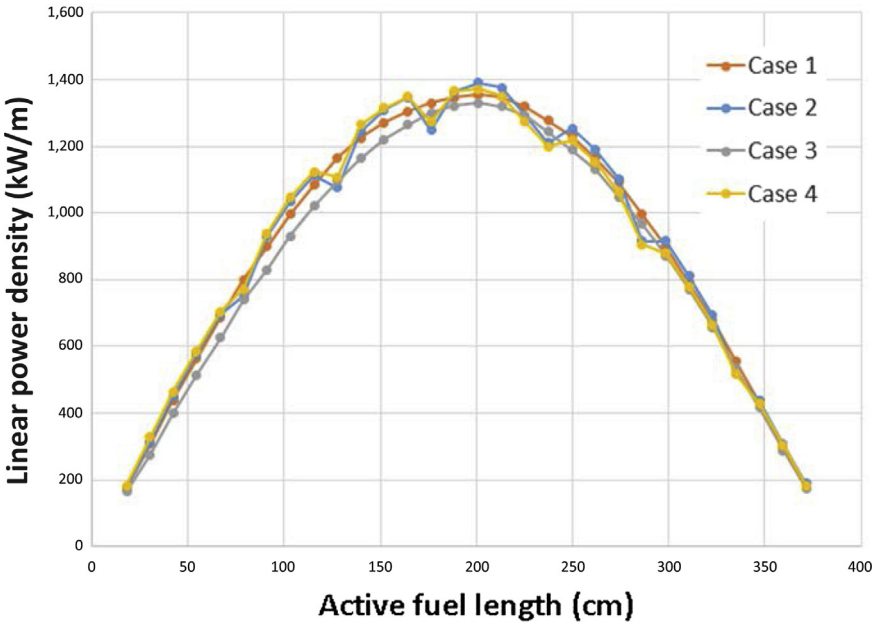

Fig. 7 – Axial power distribution in center assembly.

moderated neutrons, and this finally causes a decrease in linear power density. This can also explain the unsmooth axial power distribution of Case 4, in which the spacer grids were mixed with the moderator around their relevant positions.

Fig. 8 lets us focus on a comparison of axial power distribution in the center assembly between Case 2 (which includes the split spacer grid with a complex geometry) and Case 4 (which includes the spacer grid dissolute in the moderator only around its axial location along the assembly length). It is noted that the shape form of the linear power density in Case 2 and Case 4 are nearly the same. This is another important point in that the accuracy of the numerical results in Case 4 is reasonably acceptable.

3.4. *Neutron energy spectrum*

By tallying the neutron flux corresponding to each range of energy in the center assembly, the neutron energy spectrum was obtained as in Fig. 9.

From Fig. 9, it is difficult to see any significant differences in the neutron energy spectra of the four cases, therefore, another more detailed analysis is performed to reveal the differences. Using the neutron spectrum of Case 2 (which

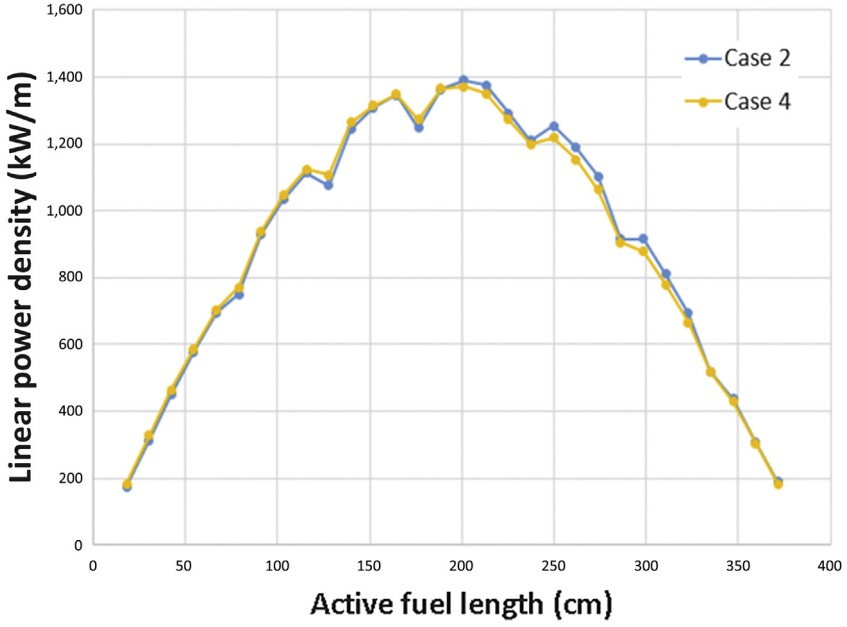

Fig. 8 – Axial power distribution in center assembly (Case 2 and Case 4).

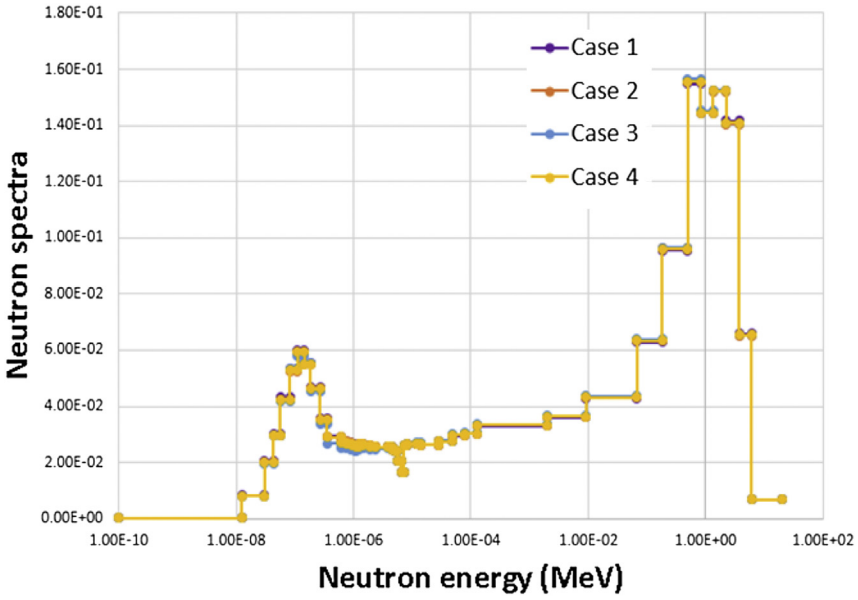

Fig. 9 – Neutron flux spectra in center assembly.

includes the split spacer grids) as the "reference", the differences between the reference spectrum and the neutron spectra of Cases 1, 3, and 4 are obtained, respectively.

Fig. 10 shows the differences of neutron spectra between Case 1 and Case 2, with no spacer grids and with spacer grids.

It is easy to realize that in the thermal energy range (< 1.00 E-6 MeV), the neutron flux of Case 1 without the spacer grids is higher than in Case 2, where the spacer grids are included. This was already explained previously (regarding multiplication factor). More moderated neutrons lead to the number of intermediate energy neutrons (from 100 eV to 1 MeV) in Case 1 to decrease and become lower than in Case 2. That is why the line representing the differences of neutron spectra "Case 1–Case 2" drops below the "zero line" (the bold black line) for the intermediate energy range, as shown in Fig. 10.

However, an interesting thing appears in the high neutron energy range (> 1 MeV). Unlike in the intermediate energy range, at this high energy range, the neutron flux of Case 1 is higher than that of Case 2. This phenomenon could be explained in the following way: In the high energy range (from 1.5 MeV to 13 MeV), Zr-90, which is the major isotope of spacer

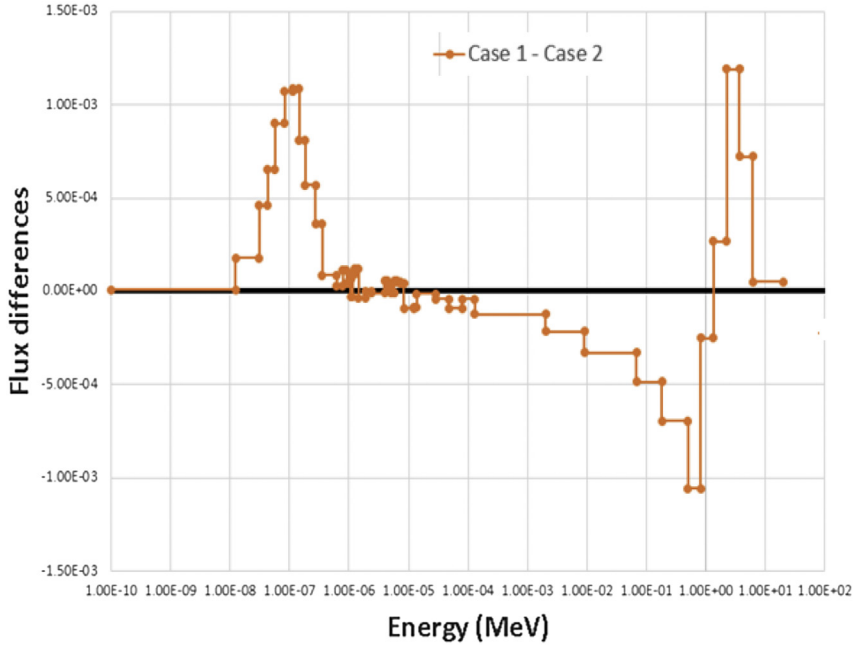

Fig. 10 – Differences of neutron flux spectra of Case 1 and Case 2 in center assembly.

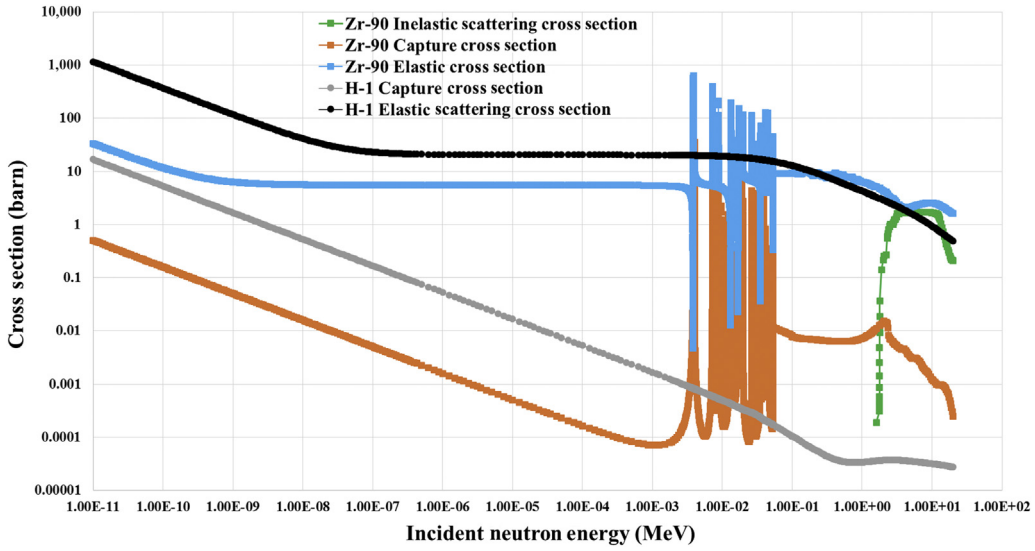

Fig. 11 – Major cross sections of Zr-90 and H-1.

grid material (Zircaloy-4), has a large inelastic scattering cross section as shown in Fig. 11, where the nuclear data is from ENDF/B-VII.1 [8]. Because of the inelastic scattering of Zr-90, high-energy neutrons are moderated to a lower energy range. Therefore, in the high-energy range, Case 2 shows a lower flux spectrum.

We will now discuss the differences in neutron spectra among the cases which include the spacer grids, but use different ways of modeling. They are Case 2 (the "volume-preserving" streamlined heterogeneous spacer grids), Case 3 (bulk dissolution spacer grids), and Case 4 (banded dissolution spacer grids). By analyzing the differences in neutron spectra, the reason for the difference in multiplication factors among the cases "without spacer grids" (as mentioned previously) can be obtained.

Fig. 12 shows that the flux differences between Case 3 and Case 2, and Case 4 and Case 2 depend on the neutron energy range in the center assembly. In the thermal energy range, the form of the grey line indicates that the neutron flux in Case 4 is higher than in Case 2, whereas the "fluctuation" of the blue line cannot be used to determine whether Case 3 or Case 2 has a higher neutron flux in this energy range. This could be explained by the fact that this "fluctuation" appears because the analysis was performed in the center assembly, which is the region that has a very low neutron flux density in the core (due to the burnable absorber), and the smaller number of thermal energy neutrons make it harder to analyze the flux differences in this energy range.

As expected, when the analysis is performed in a "hotter" assembly such as MOX-2, the flux difference between Case 3

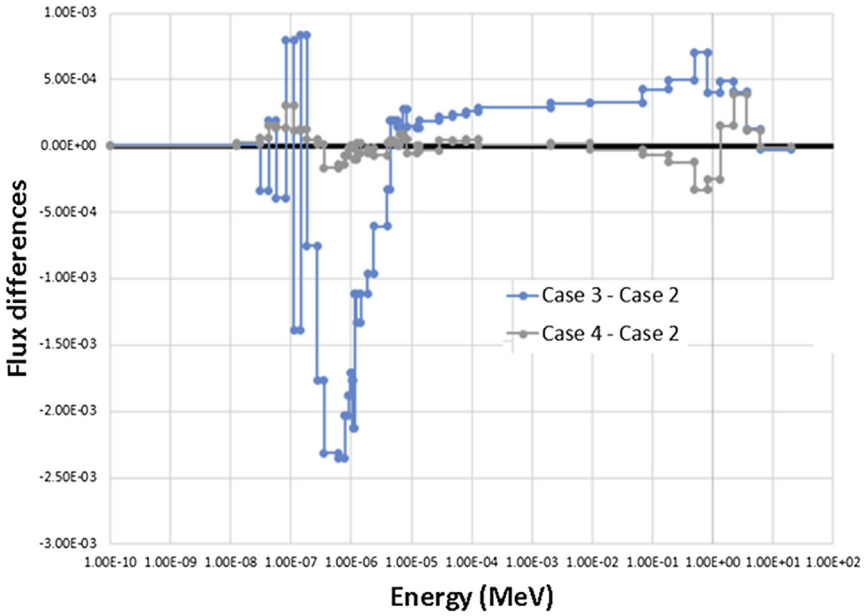

Fig. 12 – Differences of neutron flux spectra of Cases 2–4 in center assembly.

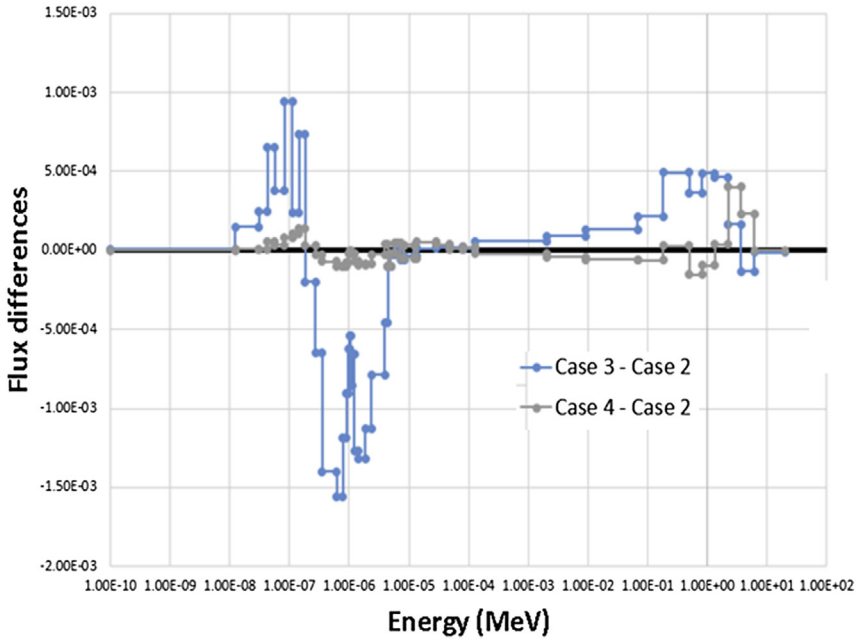

Fig. 13 – Differences of neutron flux spectra of Cases 2–4 in MOX-2 assembly.

and Case 2 in the thermal energy range is much clearer (as shown in Fig. 13).

It is clear that in Case 3, there are more thermal neutrons than in Case 2. From that, it could be concluded that the number of thermal neutrons decreases in the order: Case 3 > Case 4 > Case 2. This order corresponds to the order of multiplication factor values of the three "spacer grid included" cases (discussed previously): Case 3 (k_{eff} = 0.977060) > Case 4 (k_{eff} = 0.974790) > Case 2 (k_{eff} = 0.973620). This indicates that the thermal neutron flux seems to depend on the level of uniform distribution of spacer grid materials dissolved in the moderator of the whole core. In the "volume-preserving" streamlined heterogeneous modeling case (Case 2), the spacer grid materials are localized in a small volume (compared with the volume of the whole core moderator), and the thermal neutron flux is the lowest in this case. Similarly, when the spacer grid materials are dissolved in a larger volume, as in Case 4 and Case 3, the thermal neutron flux is higher.

4. Summary and conclusions

In this study, to investigate the effect of spacer grids in neutronics analysis, we considered four different cases of spacer grids models and compared them in the context of a modified KAIST benchmark problem 1B, using a Monte Carlo calculation. Case 1 does not include spacer grids, and the space is filled by the coolant instead. Case 2 uses the "volume-preserving" streamlined heterogeneous spacer grids which is the closest to reality. In Case 3, the spacer grids are dissolved in the moderator of the whole core (bulk dissolution model). Similarly to Case 3, Case 4 includes the spacer grids dissolved in the moderator, but only around the positions of the spacer grid along the assembly (banded dissolution model).

First, the multiplication factors of the four cases were compared. Compared to the multiplication factor of Case 2, those of Case 1 and Case 3 showed 399 pcm and 344 pcm larger values, respectively, whereas that of Case 4 showed 117 pcm larger values. This means that the multiplication factor can be significantly larger when the spacer grids are simply replaced with the moderator. In addition, as the spacer grids are dissolved in the moderator more uniformly, the multiplication factor increases.

Second, the effects of spacer grids in axial and radial flux distributions were also analyzed. In Case 2 and Case 4, it is clearly seen that the flux distributions decrease at the positions of the spacer grids, whereas Case 1 and Case 3 do not show these tendencies. Comparisons of the flux spectra also show that Case 4 yields the closest spectrum to Case 2 among the cases considered in this study.

In conclusion, for the Monte Carlo calculation, which can handle complex geometry, Case 2 (volume-preserving streamlined heterogeneous spacer grids model) is recommended. However, for the deterministic calculation in which it is not easy to describe complex geometry, Case 4 (banded dissolution model) is recommended. It should be noted though that Case 4 provides around a 100 pcm higher multiplication factor than Case 2.

Conflicts of interest

All authors have no conflicts of interest to declare.

Acknowledgments

The authors would like to express their gratitude to YuGwon Jo of KAIST for his enthusiastic help during this study. The first author (X.B. Tran) would also like to thank the Korea Institute of Nuclear Safety, as well as the Korean and Vietnamese governments for all the support and favorable conditions provided during his stay in Korea.

REFERENCES

[1] X-5 MONTE CARLO TEAM, MCNP – A General N-Particle Transport Code, Version 5-Volume I: Overview and theory, LA-UR-03-1987, Los Alamos National Laboratory, 2003.

[2] KNF-TRDMR-04001/N/A Rev. 0, PLUS7 Fuel Design and Safety Evaluation for Korean Standard Nuclear Power Plants, 2006.

[3] A. Pazirandeh, S. Ghaseminejad, M. Ghaseminejad, Effects of various spacer grid modeling on the neutronic parameters of the VVER-1000 reactor, Ann. Nucl. Energy 38 (2011) 1978–1986.

[4] KAIST-Benchmark Problem 1B [Internet]. Available from: http://nurapt.kaist.ac.kr/benchmark/contents.htm.

[5] Y.H. Kim, K.T. Kim, Advanced spacer grid design for PLUS7 fuel assembly, In Proceedings of Korean Nuclear Society Meeting, Yongpyong, Korea October 24–25, 2002.

[6] A.T. Godfrey, VERA Core Physics Benchmark Progression Problem Specifications – Revision 2, CASL, March 29, 2013.

[7] A. Rubin et al., OECD/NRC BENCHMARK Based on NUPEC PWR Subchannel and Bundle Tests (PSBT), US NRC OECD Nuclear Energy Agency, November 2010.

[8] M.B. Chadwick et al., ENDF/B-VII.1 nuclear data for science and technology: cross sections, covariances, fission product yields and decay data, Nucl. Data Sheets 112 (2011) 2887–2996.